Research Square

Preprints are preliminary reports that have not undergone peer review.
They should not be considered conclusive, used to inform clinical practice,
or referenced by the media as validated information.

Aqueous Humor Proteomic Analysis Identifies Diagnostic Biomarkers for Autoimmune Optic Neuritis

qingyuan mao
Affiliated Hospital of Nantong University
min zhang
Affiliated Hospital of Nantong University
shiyu huang
Affiliated Hospital of Nantong University
junfang zhang
Affiliated Hospital of Nantong University
jiawei luo
Affiliated Hospital of Nantong University
hongwei gu
Affiliated Hospital of Nantong University
huaijin guan
Affiliated Hospital of Nantong University
min ji
amyj1234@163.com
Affiliated Hospital of Nantong University

Research Article

Keywords: autoimmune optic neuritis, data-independent acquisition, aqueous humor, biomarker, lactoferrin

Posted Date: November 5th, 2026

DOI: https://doi.org/10.21203/rs.3.rs-11055905/v1

License: This work is licensed under a Creative Commons Attribution 4.0 International License. Read Full License

Additional Declarations: No competing interests reported.

Abstract

Autoimmune optic neuritis (AON) is an inflammatory optic neuropathy that commonly presents with acute or subacute visual loss. In the early stage, AON may overlap clinically with other optic neuropathies, particularly non-arteritic anterior ischemic optic neuropathy (NAION). Although serum and cerebrospinal fluid biomarkers can provide diagnostic assistance, they do not directly reflect the local ocular microenvironment. In this study, aqueous humor (AH) was used as a local liquid biopsy source to identify candidate molecules associated with AON. Data-independent acquisition (DIA) proteomics was applied to analyze AH proteins obtained from patients with AON, patients with NAION, and presbyopic surgical controls (CTL group) during anterior chamber paracentesis or surgery. Candidate biomarkers were subsequently quantified by enzyme-linked immunosorbent assay (ELISA).

Proteomic analysis identified 4,264 proteins from 18 samples. Gene Ontology annotation and functional analysis showed that AON-related biological processes were mainly associated with immune responses, ganglioside biosynthesis, glycoprotein biosynthesis, lysosomal function, and protein translation. Candidate protein selection integrated fold change, biological module relevance, protein-protein interaction (PPI) network centrality, and ELISA feasibility, leading to the selection of lactoferrin (LTF), ribosomal protein SA (RPSA), and ATPase H+ transporting V1 subunit A (ATP6V1A) for further validation. The results showed that LTF concentration differed significantly between the AON and CTL groups and demonstrated diagnostic utility in receiver operating characteristic analysis, suggesting that LTF may serve as a potential aqueous humor biomarker for AON. In contrast, RPSA and ATP6V1A did not show stable intergroup differences during validation; nevertheless, the protein translation stress and lysosome-related pathways represented by these molecules suggest corresponding functional alterations in the AH microenvironment of AON. Overall, this study provides an initial characterization of the AH proteomic profile in AON and indicates that AH proteomics may offer a new approach for elucidating local pathological mechanisms and identifying fluid-based diagnostic biomarkers for AON.

Introduction

Optic neuritis is a potentially sight-threatening optic nerve disorder characterized primarily by inflammatory injury[1, 2]. It typically manifests as acute or subacute visual loss, pain with eye movement, color vision impairment, and visual field defects. The disease occurs predominantly in young and middle-aged adults and can substantially affect visual function and quality of life[3, 4]. Epidemiological studies have reported an annual incidence of approximately 0.56 to 5.36 cases per 100,000 individuals, with most cases occurring between 20 and 50 years of age and with a relative female predominance[3]. With advances in neuroimmunology and ophthalmic imaging, the contribution of autoimmune mechanisms to optic neuritis has received increasing attention[1, 2]. As an important form of optic neuritis, AON exhibits clinical heterogeneity, and some patients may experience severe visual impairment or a high risk of relapse. Therefore, early recognition and timely intervention are clinically important. However, early AON may overlap with other optic neuropathies, especially NAION, in terms of acute visual decline, optic disc edema, and visual field loss[5–7]. Although serum testing, cerebrospinal fluid examination, imaging, and clinical symptom assessment can support diagnosis, limitations remain in antibody-negative patients, atypical presentations, or inconsistent test results[8–13].

Pathologically, AON is mainly associated with immune-mediated inflammation of the optic nerve, myelin injury, increased blood-nerve barrier permeability, and secondary axonal damage[1, 2, 8–10]. In the acute phase, inflammatory cell infiltration and mediator release may induce optic nerve edema, impair axoplasmic transport, and interfere with nerve conduction, resulting in visual dysfunction. If inflammation persists or injury is severe, progressive retinal nerve fiber loss, optic atrophy, and irreversible visual impairment may occur. Unlike ischemic optic neuropathy, which is primarily characterized by acute hypoperfusion, AON is dominated by immune inflammation and the resulting demyelinating and neural tissue injury[7]. Nevertheless, the two conditions may show overlapping early clinical manifestations, making accurate differentiation difficult when based solely on symptoms and routine ophthalmic examination. Thus, capturing AON-

related inflammatory and tissue-injury signals at the level of the ocular microenvironment may provide new evidence for diagnosis and mechanistic investigation.

Aqueous humor is an intraocular fluid produced by the ciliary body and circulated through the posterior and anterior chambers. It is involved in maintaining intraocular pressure, nourishing avascular ocular tissues, clearing metabolic products, and regulating the intraocular immune microenvironment[14, 15]. Compared with serum and cerebrospinal fluid, AH is anatomically closer to ocular tissues. Alterations in its proteins, cytokines, growth factors, and metabolism-related molecules can partly reflect blood-ocular barrier disruption, local inflammation, and tissue injury. Although the amount of AH that can be obtained is limited, it can be collected during anterior chamber paracentesis or intraocular surgery, and it is more accessible and less invasive than vitreous humor or cerebrospinal fluid, with considerable translational potential[14, 16]. Previous studies have shown that AH protein composition changes in glaucoma, diabetic retinopathy, age-related macular degeneration, uveitis, and other ocular diseases, and these changes can be used to explore disease mechanisms and candidate biomarkers[14–19]. However, AH molecular studies in AON remain scarce, and whether AH can reflect AON-related intraocular immune abnormalities and distinguish them from other optic neuropathies remains to be clarified.

Proteomics provides a powerful approach for characterizing complex protein mixtures in body fluids and discovering disease biomarkers[20]. In recent years, advances in liquid chromatography-tandem mass spectrometry and data-independent acquisition have enabled deep quantitative analysis of low-abundance, low-volume samples. DIA provides high-throughput and reproducible protein quantification and is particularly suitable for discovery-phase studies of small-volume body fluids such as AH.

The present study enrolled patients with AON, patients with NAION, and presbyopic surgical controls. DIA proteomics was used to analyze differences in AH protein expression profiles, and bioinformatics analysis was applied to screen AON-related candidate proteins[21, 22]. These candidates were then validated by ELISA to evaluate their potential value for AON diagnosis and differential diagnosis[16]. This study aimed to investigate AON-related molecular changes from the perspective of local ocular liquid biopsy and to provide experimental evidence for early recognition, disease mechanism research, and subsequent biomarker development in AON.

Materials and Methods

Patients and Controls

This study enrolled 27 patients with AON, 21 patients with NAION, and 13 control patients undergoing presbyopia-related surgery at the Eye Center of the Affiliated Hospital of Nantong University between November 2023 and January 2026. Before enrollment, all participants underwent basic medical history collection and routine ophthalmic examinations. Group allocation was performed by experienced ophthalmologists based on clinical manifestations, fundus findings, imaging data, and relevant ancillary examinations. The study was conducted in accordance with the Declaration of Helsinki and was approved by the Ethics Committee of the Affiliated Hospital of Nantong University. Written informed consent was obtained from all participants or their legal representatives after a full explanation of the study purpose, sampling procedures, and potential risks.

The AON group included first-episode patients with a disease duration of no more than 3 months who met the 2022 international diagnostic criteria for optic neuritis[2]. The NAION group included first-episode patients with a disease duration of no more than 3 months who met the Chinese expert consensus criteria for the diagnosis and treatment of NAION[7]. The CTL group consisted of patients undergoing presbyopia-related surgery without obvious optic neuropathy, active intraocular inflammation, or severe systemic immune disease. Common exclusion criteria included previous ocular

surgery or trauma, coexisting ocular or neurological diseases that could interfere with the interpretation of visual function, refractive error of 6.0 diopters or more in absolute value, intraocular pressure greater than 21 mmHg, and treatment with glucocorticoids or immunosuppressants within 30 days before sampling.

For proteomic analysis, AH samples were processed independently at the individual-sample level, with 6 participants included in each group. For candidate protein validation, 43 available AH samples with sufficient volume and quality were analyzed by ELISA, including 21 samples from the AON group, 15 from the NAION group, and 7 from the CTL group. The main clinical characteristics of the discovery and validation cohorts are presented in Table 1.

Table 1
Clinical characteristics of participants in the discovery and validation sets

Characteristics	Discovery set				Validation set			
	AON(n = 6)	NAION(n = 6)	CTL(n = 6)	p value	AON(n = 21)	NAION(n = 15)	CTL(n = 7)	p value
Sex,male/female	2/4	1/5	1/5	0.8	11/10	9/6	5/2	0.7
Age,years	48(44–60)	57(50–64)	61(54–74)	0.1	46(28–66)	54(44–78)	62(53–75)	0.2
BCVA,logMAR	0.76(0.22-2.00)	0.45(0.22-2.00)	0.40(0.30–0.52)	0.6	0.88(0.22-2.00)	0.54(0.22-2.00)	0.38(0.28–0.66)	0.4
IOP,mmHg	14(10–16)	13(11–19)	17(15–20)	0.1	13(10–17)	14(10–19)	14(12–20)	0.2
Hypertension	1(17)	3(50)	2(33)	0.5	4(19)	10(66)	3(42)	0.2
Diabetes	0(0)	2(33)	1(17)	0.5	0(0)	3(20)	0(0)	0.3
Hyperlipidemia	1(17)	2(33)	0(0)	0.4	2(17)	4(26)	1(14)	0.4
AQP4-IgG	3(50)	NA	NA	NA	5(23)	NA	NA	NA
MOG-IgG	0(0)	NA	NA	NA	7(33)	NA	NA	NA

Values are presented as median (range) or number (%), unless otherwise indicated. p values compare the three groups within each set. AON, autoimmune optic neuritis; NAION, non-arteritic anterior ischemic optic neuropathy; CTL, control; BCVA, best-corrected visual acuity; IOP, intraocular pressure; AQP4-IgG, aquaporin-4 immunoglobulin G; MOG-IgG, myelin oligodendrocyte glycoprotein immunoglobulin G; NA, not applicab

Clinical Examinations and Collection of Serum and Aqueous Humor Samples

All participants underwent standardized clinical data collection, including age, sex, systemic disease history, ocular history, disease onset time, and previous treatment. Ophthalmic examinations included best-corrected visual acuity, intraocular pressure, relative afferent pupillary defect testing, slit-lamp biomicroscopy, dilated fundus examination, fundus photography, visual field testing, and visual evoked potential testing. When clinically indicated, patients with AON or NAION underwent brain and orbital magnetic resonance imaging or contrast-enhanced MRI to evaluate optic nerve involvement and exclude compressive, infectious, or other non-target optic neuropathies.

Peripheral serum was routinely collected from patients with AON on the day of admission for testing of antibodies related to central nervous system demyelinating diseases. A target-based assay combined with a cell-based assay was used to detect AQP4-IgG, MOG-IgG, and GFAP-IgG. AH samples were collected under strictly sterile conditions. In the AON and NAION groups, AH was obtained by anterior chamber paracentesis under slit-lamp guidance, whereas in the CTL group it

was collected at the beginning of surgery before anterior chamber manipulation. Approximately 50 to 100 microliters of AH was collected from each case and immediately processed under low-temperature conditions. Samples were centrifuged at 10,000 g for 10 min at 4 degrees Celsius, and the supernatants were transferred into sterile enzyme-free Eppendorf tubes, coded, and stored at -80 degrees Celsius until proteomic analysis or ELISA validation.

Aqueous Humor Proteomic Analysis

A discovery DIA proteomic strategy was used to perform in-depth analysis of AH proteins.The overall experimental workflow of the discovery and validation phases is illustrated in Fig. 1. Similar to the workflow in reference proteomic studies that use separate discovery and validation cohorts, the present study first performed unbiased protein profiling of AH samples, then identified candidate proteins based on bioinformatics analysis, and finally validated these proteins in independent available samples using ELISA. Unlike some proteomic studies of low-abundance body fluids that use pooled samples, all samples in the DIA analysis were processed individually for protein extraction, digestion, mass spectrometric acquisition, and database searching, in order to preserve interpatient biological variation and reduce the masking of individual differences caused by pooling.

Protein Extraction and Low-Abundance Protein Enrichment

AH samples were removed from − 80 degrees Celsius storage and slowly thawed on ice. The samples were centrifuged at 15,000 g for 10 min at 4 degrees Celsius to remove cellular debris and small particulate impurities. The supernatants were transferred to ultrafiltration devices and concentrated to a final volume of approximately 40 microliters. To improve the detection of low-abundance proteins, the concentrated samples were mixed thoroughly with an equal volume of phosphate-buffered saline and incubated with a magnetic bead system at room temperature under agitation to allow sufficient protein binding. After incubation, the tubes were placed on a magnetic rack until the beads were completely adsorbed onto the tube wall. The supernatant was discarded, and the beads were washed 2 to 3 times to reduce salts, lipids, and other interfering components. Proteins were then exchanged and dissolved in 8 M urea, and the protein concentration was determined by bicinchoninic acid assay for subsequent equal loading and digestion.

Protein Digestion and Peptide Preparation

According to the measured protein concentration, equal amounts of protein from each sample were subjected to digestion. Samples were first precipitated with trichloroacetic acid and washed with prechilled acetone to remove impurities that could affect trypsin digestion and mass spectrometric detection. After drying, the precipitates were resuspended in an appropriate buffer. Dithiothreitol was added for reduction to fully open disulfide bonds, followed by alkylation with iodoacetamide to stabilize cysteine residues and reduce modification-related uncertainty during identification. Trypsin was then added at the defined ratio, and digestion was performed overnight at 37 degrees Celsius. The digestion reaction was terminated by acidification, and peptides were desalted using solid-phase extraction columns. The desalted peptides were vacuum dried, reconstituted, and quantified with a peptide quantification kit to ensure relatively consistent peptide input before mass spectrometry.

Liquid Chromatography-Tandem Mass Spectrometry

Peptide samples were separated using a nano-flow liquid chromatography system and analyzed by a high-resolution mass spectrometer in DIA mode. The mass spectrometer was operated in positive ion mode, with a precursor ion scan range of 380 to 980 m/z. The MS1 resolution was set at 240,000 at 200 m/z, the normalized AGC target was 500%, and the maximum injection time was 5 ms. MS2 spectra were acquired in DIA mode using 299 scan windows, with an

isolation window of 2 m/z, higher-energy collisional dissociation collision energy of 25 eV, normalized AGC target of 500%, and maximum injection time of 3 ms. This acquisition strategy systematically records peptide fragment ion information within predefined mass windows and offers better quantitative consistency and data completeness than conventional data-dependent acquisition. It is therefore suitable for clinical AH samples, which are small in volume, low in protein abundance, and characterized by marked interindividual variability.

Data Processing and Differential Protein Screening

Raw DIA data were processed with DIA-NN for database searching and protein quantification. The search parameters were set as follows: trypsin digestion, a maximum of 1 missed cleavage, carbamidomethylation of cysteine as a fixed modification, and oxidation of methionine and acetylation of the protein N terminus as variable modifications. A false discovery rate below 1% was applied at both the protein and peptide levels. After database searching, quality control was performed for peptide length distribution, identified peptide number, missed cleavage rate, and protein quantification consistency to ensure that subsequent differential analysis was based on stable and reliable data. In this study, most identified peptides were 7 to 20 amino acids long, consistent with the expected pattern of tryptic digestion and mass spectrometric fragmentation.

For differential protein screening, protein quantitative data from all samples were first normalized, and intergroup fold changes were calculated. For each comparison, the relative quantitative value of each protein within the group was used to calculate expression differences between AON and NAION and between AON and CTL. Proteins with a p value below 0.05 and fold change above 1.3 were defined as significantly upregulated, whereas those with a p value below 0.05 and fold change below 1/1.3 were defined as significantly downregulated. Differentially expressed proteins were then used for volcano plots, clustering analysis, functional enrichment, and PPI network analysis to characterize the AH proteomic profile associated with AON.

Functional Annotation, Enrichment Analysis, and PPI Network Construction

To interpret the biological processes reflected by the differentially expressed proteins, eggnog-mapper was used for Gene Ontology annotation of the identified proteins, which were categorized into biological process, molecular function, and cellular component terms. KEGG pathway annotation was performed based on database matching, and the highest-scoring match for each protein sequence was selected as the pathway annotation. All proteins identified in this study were used as the background for enrichment analysis. Fisher exact tests were used to assess enrichment of differentially expressed proteins in GO terms and KEGG pathways, and p values below 0.05 were considered statistically significant.

For PPI network analysis, database identifiers or protein sequences corresponding to the differentially expressed proteins were submitted to the STRING database, and a confidence score greater than 0.7 was used as the threshold for high-confidence interactions. The interaction network was then visualized using the visNetwork package in R. Fold change, statistical significance, functional module relevance, and network topology were jointly considered to further identify core candidate proteins potentially involved in changes in the AH microenvironment of AON. This step was designed not merely to list differential proteins, but to link expression changes with immune responses, protein synthesis, glycoprotein biosynthesis, lysosomal function, and other related biological processes, thereby providing a basis for subsequent targeted validation.

Candidate Protein Selection and ELISA Validation

Candidate proteins were selected according to four criteria. First, the protein had to show clear expression changes in AON compared with the control group or NAION. Second, the functional module containing the protein had to be

biologically related to inflammation, immune responses, cellular stress, protein synthesis, or lysosome-related processes potentially involved in AON. Third, the protein had to show a certain degree of connectivity in the PPI network or be located within a key functional module. Fourth, the protein had to be suitable for commercial ELISA detection, allowing validation in limited-volume AH samples. Based on these criteria, LTF, RPSA, and ATP6V1A were selected as candidate proteins.

ELISA validation was performed using independent available AH samples, including 21 from the AON group, 15 from the NAION group, and 7 from the CTL group. All assays were conducted strictly according to the manufacturer instructions. Before the experiment, samples were thawed on ice and thoroughly mixed. Standards, quality controls, and test samples were added according to the kit protocol. After incubation, washing, enzyme-conjugate reaction, substrate color development, and reaction termination, absorbance was measured using a multifunctional microplate reader. Candidate protein concentrations were calculated from standard curves. To reduce interplate and operational variability, each candidate protein was measured under similar experimental conditions whenever possible, and results that were clearly abnormal or failed quality control were excluded before data analysis.

Statistical Analysis

Statistical analyses were performed using SPSS version 27.0. The Shapiro-Wilk test was first used to assess whether continuous variables followed a normal distribution. Normally distributed data were expressed as mean ± standard deviation and compared using independent-samples t tests or one-way analysis of variance. Non-normally distributed data were expressed as medians with ranges and compared using Mann-Whitney U tests or Kruskal-Wallis tests. Categorical variables were expressed as numbers and percentages and compared using Fisher exact tests. Candidate protein concentrations obtained from ELISA validation were used for intergroup comparisons. Receiver operating characteristic curves were further used to evaluate the discriminative performance of candidate proteins for AON or optic neuropathy-related grouping, and the area under the curve and 95% confidence intervals were calculated. A p value below 0.05 was considered statistically significant.

Results

The baseline clinical characteristics of participants in the discovery and validation cohorts were first compared. The discovery cohort included 6 AON patients, 6 NAION patients, and 6 CTL participants for AH DIA proteomic analysis. The validation cohort included 21 AON patients, 15 NAION patients, and 7 CTL participants for ELISA-based quantification of candidate proteins. In the discovery cohort, no significant differences were observed among the AON, NAION, and CTL groups in sex, age, best-corrected visual acuity, intraocular pressure, hypertension, diabetes, or hyperlipidemia (all $p > 0.05$). In the AON group, 3 patients were AQP4-IgG positive, whereas no MOG-IgG-positive cases were observed. In the validation cohort, the overall distribution of clinical characteristics was also balanced across groups, providing a relatively comparable clinical basis for subsequent proteomic discovery and candidate protein validation.

Proteomic Quality Control, Intergroup Differences, and Differentially Expressed Protein Screening

During the discovery phase, DIA proteomics was used to analyze AH protein expression profiles in the AON, NAION, and CTL groups. After database searching and quality control, 4,264 proteins were identified.The quality control metrics, principal component analysis, volcano plots, and heatmaps are summarized in Fig. 2. Peptide length distribution was mainly concentrated between 7 and 20 amino acids, and non-missed-cleavage peptides accounted for the majority, consistent with the expected characteristics of tryptic digestion and mass spectrometric identification. These findings indicate that the proteomic dataset was technically reliable.

To further evaluate differences in the global protein expression profiles among the three groups, principal component analysis was performed for unsupervised dimensionality reduction. The PCA plot showed partial separation among AON, NAION, and CTL samples. NAION and CTL samples showed relatively clear intragroup clustering, whereas AON samples exhibited a wider distribution, suggesting stronger interindividual heterogeneity in the AH proteomic profile of AON. Overall, the three groups could be distinguished at the proteomic level, supporting subsequent differential protein screening and mechanistic analysis.

Based on intergroup differences in protein expression, differentially expressed proteins were further screened between AON and NAION and between AON and CTL. Using p value and fold change as screening criteria, 391 differentially expressed proteins were identified between the AON and NAION groups, including 186 upregulated and 205 downregulated proteins. Between the AON and CTL groups, 341 differentially expressed proteins were identified, including 202 upregulated and 139 downregulated proteins. These results indicate that the AH proteomic profile of AON differs not only from that of normal controls but also from that of ischemic optic neuropathy at the molecular level.

Volcano plots showed that ATP6V1A, ANXA8L1, and ALDH3A1 were relatively upregulated in AON compared with NAION, whereas VGF, INHBA, and CPXM2 were relatively downregulated. In the comparison between AON and CTL, LTF, THSD4, RPL35, and HNRNPA2B1 showed upregulation, whereas LRRC24 and LMAN1 showed downregulation. Hierarchical clustering heatmaps further demonstrated that samples from AON and NAION and those from AON and CTL could form distinct clustering patterns based on the expression levels of differentially expressed proteins, suggesting that these proteins capture molecular differences between AON and other comparison states.

Functional Annotation and Enrichment Analysis of Differential Proteins

To elucidate the biological processes associated with AON-related differentially expressed proteins, GO functional annotation and KEGG pathway enrichment analyses were performed.The detailed GO annotations and KEGG pathway enrichment networks are presented in Fig. 3. GO annotation indicated that AON-related differential proteins were involved in biological process, cellular component, and molecular function categories. In the comparison between AON and NAION, differential proteins were mainly enriched in translation, immune response, protein localization, cellular process, metabolic process, and biological regulation. In the comparison between AON and CTL, cell adhesion, secretory granule lumen, extracellular matrix, and protein binding were also prominent.

KEGG enrichment analysis further showed that AON-related differential proteins were involved in multiple metabolic and cellular functional pathways. In the comparison between AON and NAION, differential proteins were enriched in glycosaminoglycan degradation, cholesterol metabolism, sphingolipid metabolism, and glycoprotein-related processes. In the comparison between AON and CTL, lysosomes, glycoprotein biosynthesis, and ganglioside biosynthesis also showed strong enrichment trends.

These results suggest that AH proteomic changes in AON are not limited to isolated inflammatory proteins, but rather involve coordinated alterations in immune response, protein synthesis and transport, glycoprotein processing, lysosomal function, and lipid metabolism. Immune and lysosome-related processes may be associated with inflammatory cell activation, antigen processing, and changes in the local immune microenvironment, whereas enrichment of ribosomal and translation-related proteins suggests alterations in local protein synthesis and stress responses in the pathological state of AON.

PPI Network Analysis and Core Protein Screening

To identify key regulatory nodes among AON-related differential proteins in AH, a PPI network was constructed based on differentially expressed proteins, and core proteins were screened according to node connectivity.The PPI networks and

the core protein modules are displayed in Fig. 4 The PPI network showed relatively concentrated interaction modules in both the AON versus NAION and AON versus CTL comparisons, suggesting that some differential proteins may serve as central nodes in AON-associated molecular networks.

In the comparison between AON and NAION, core proteins were mainly enriched in the ribosomal protein family, including RPS3, RPS16, RPSA, RPS3A, RPS13, RPS19, RPS4X, RPS11, and RPS23, along with receptor for activated C kinase 1. These findings indicate that ribosome-related proteins may represent important nodes in the differential protein network between AON and NAION. In the comparison between AON and CTL, core proteins also involved ribosomal proteins, translation-related proteins, and molecules related to cytoskeleton or protein processing. These findings suggest that AH proteomic changes in AON may reflect not only inflammatory responses, but also cellular stress, protein processing, and compensatory responses after local tissue injury.

ELISA Validation of Candidate Proteins

Based on fold change, functional enrichment modules, biological significance, PPI network centrality, and ELISA feasibility, LTF, RPSA, and ATP6V1A were selected as candidate proteins for further validation.The ELISA validation results and the corresponding ROC curve analyses for the three candidate proteins are shown in Fig. 5 ELISA results showed that LTF expression levels were higher in both the AON and NAION groups than in the CTL group. The difference between the AON and CTL groups was statistically significant, and the difference between the NAION and CTL groups was also significant, whereas the difference between AON and NAION did not reach statistical significance. These findings suggest that LTF may reflect optic neuropathy-related inflammation or tissue injury and may be more appropriately considered a fluid biomarker associated with optic nerve disease.

In contrast, RPSA and ATP6V1A did not show stable significant differences among the three groups. Although these proteins showed certain differential or network relevance in the discovery proteomic analysis, they did not demonstrate clear diagnostic discrimination in independent-sample validation. This finding suggests that candidate proteins identified through discovery proteomics require further filtering at the individual-sample level, and only molecules with stable differences during validation are more likely to have translational value.

ROC curve analysis further evaluated the diagnostic performance of the candidate proteins. In the comparison between AON and CTL, the area under the curve for LTF was 0.816, with a 95% confidence interval of 0.577 to 0.954. In the comparison between NAION and CTL, the area under the curve for LTF was 0.848, with a 95% confidence interval of 0.613 to 0.979, indicating that LTF had a certain diagnostic value in distinguishing optic neuropathy from the control state. In comparison, RPSA and ATP6V1A showed weaker ROC performance and no clear independent diagnostic advantage.

Discussion

In this study, DIA-based AH proteomics was used to compare the protein expression profiles of patients with AON, patients with NAION, and control participants, followed by ELISA validation of candidate proteins in independent samples. Overall, clear differences in AH protein expression were observed between AON and NAION and between AON and CTL. The differentially expressed proteins were mainly related to immune responses, protein synthesis, glycoprotein biosynthesis, lysosomal function, and stress-associated processes. Further validation showed that LTF had favorable discriminative performance in comparisons of AON versus CTL and NAION versus CTL, whereas RPSA and ATP6V1A, although relevant at the network or pathway level in the discovery phase, did not show stable differences in ELISA validation. These findings suggest that molecular changes in the AH of AON may include both shared responses related to inflammatory optic neuropathy and disease-related molecular modules that require further screening and validation.

The diagnosis of optic neuritis has long relied on clinical presentation, imaging findings, and serum or cerebrospinal fluid markers[1, 2, 8–10]. In recent years, studies of AQP4-IgG, MOG-IgG, neurofilament light chain, and glial fibrillary acidic protein have refined the diagnosis and stratification of optic neuritis. However, these markers primarily reflect systemic immune status, central nervous system injury, or glial responses, and they may not directly capture the local intraocular microenvironment[14, 15]. In contrast, AH is anatomically closer to ocular tissues and contains proteins, growth factors, immune molecules, and metabolic components that can partly reflect blood-ocular barrier disruption, local inflammation, and tissue injury. Previous studies of the human AH proteome have shown that, despite the small sample volume and low protein concentration, LC-MS/MS-based approaches can generate rich proteomic information and support mechanistic and biomarker studies in glaucoma, diabetic retinopathy, uveitis, and other ocular diseases[17–19]. Therefore, using AH as a local ocular liquid biopsy sample in AON has both technical feasibility and clinical translational significance.

A total of 4,264 AH proteins were identified in this study, with 391 differentially expressed proteins between AON and NAION and 341 between AON and CTL. These findings indicate broad proteomic remodeling in AON. Previous AH proteomic studies of diabetic retinopathy have shown that disease progression is accompanied by gradual changes in immune response, lipid metabolism, complement activation, and vascular-related pathways, and that certain AH proteins are associated with disease severity, treatment response, and complication development[16]. Proteomic studies of AH and vitreous humor in inflammatory ocular diseases such as uveitis have also suggested that complement cascades, acute-phase responses, inflammatory mediator release, and increased vascular permeability are common molecular features of intraocular inflammation[19]. These findings are broadly consistent with the enrichment of immune response, glycoprotein biosynthesis, and lysosome-related pathways observed in the present study, supporting the use of AH proteomics as a window into intraocular inflammation and tissue injury.

From a pathological perspective, AON is mainly associated with immune-mediated optic nerve inflammation, demyelinating injury, blood-nerve or blood-ocular barrier disruption, and secondary axonal damage, whereas NAION is primarily associated with acute hypoperfusion of the optic nerve head and ischemia-reperfusion injury. The two conditions can overlap clinically in acute visual loss, optic disc edema, and visual field defects, but their initiating mechanisms and tissue injury patterns differ[8–10]. Therefore, the presence of differential proteomic profiles between AON and NAION is consistent with their distinct pathological bases. Notably, not all differential proteins should be interpreted as AON-specific molecules, because acute optic nerve injury may commonly induce barrier breakdown, inflammation, protein extravasation, and local repair processes. The simultaneous inclusion of both NAION and CTL groups in this study helps to preliminarily distinguish shared responses of optic neuropathy from AON-related changes, although larger sample sizes and longitudinal data are needed to define disease specificity more clearly.

Functional enrichment analysis showed that AON-related differential proteins were involved in translation, ribosomes, protein processing, and glycoprotein biosynthesis. Previous studies have indicated that ribosomal proteins not only participate in protein translation but also exert diverse extra-ribosomal functions, including regulation of cellular stress, DNA damage responses, cell proliferation, apoptosis, and immune signaling[23, 24]. Under inflammatory or injury conditions, local cells may exhibit altered protein synthesis requirements, translational remodeling, and release of stress-associated proteins. Therefore, it is not unexpected that ribosome-related proteins formed a concentrated PPI network in this study. RPSA, in particular, is not only a ribosomal protein but is also related to the 37/67-kDa laminin receptor, which participates in cell adhesion, migration, and interactions with the extracellular matrix. Considering the changes in extracellular matrix[25, 26], protein binding, and translation-related pathways observed in this study, the inclusion of RPSA as a candidate protein in the discovery phase was biologically plausible.

However, RPSA did not show stable differences in ELISA validation, suggesting that it may represent network centrality or pathological module changes in the discovery phase rather than a reliable standalone fluid diagnostic biomarker. Several factors may account for this discrepancy. First, many ribosomal proteins are intracellular proteins, and their detectable

changes in AH may be influenced by cell disruption, timing of release, sample handling, and the stability of low-abundance detection. Second, AON patients may vary in disease duration, inflammatory activity, and antibody status, resulting in substantial interindividual fluctuations in RPSA levels. Third, discovery proteomics and ELISA validation differ in detection principles, antibody recognition epitopes, and dynamic ranges, and some proteins that appear differential in mass spectrometry may not be fully reproduced by immunoassays. Thus, the negative validation result for RPSA does not negate the relevance of ribosome-related pathways in AON, but it indicates that single ribosomal proteins should be interpreted cautiously as clinical biomarkers.

ATP6V1A was also selected as a candidate protein for validation. ATP6V1A is an important subunit of the V1 domain of vacuolar H+ ATPase and is involved in lysosomal acidification, intracellular pH homeostasis, endosomal function, and autophagolysosomal activity[27–30]. Previous studies have shown that V-ATPase not only maintains organelle acidification but also participates in autophagy, mTOR signaling, cell death, and immune regulation. In studies of neurodegenerative diseases and immune cell function, impaired lysosomal acidification has been closely associated with cellular stress, amplification of inflammation, and metabolic abnormalities[29, 30]. Therefore, the enrichment of lysosomal and protein degradation pathways in this study suggests that the local ocular environment of AON may involve lysosomal functional alterations related to antigen processing, inflammatory cell activation, or clearance of damaged proteins.

Similar to RPSA, ATP6V1A did not show stable intergroup differences in subsequent ELISA validation. This result suggests that lysosome-related changes may be expressed more as pathway-level disturbances than as stable increases or decreases in a single V-ATPase subunit. Another possibility is that ATP6V1A mainly resides in intracellular structures, and its detectable level in AH may be low and influenced by cell origin, release mode, and protein stability. Therefore, in future studies, ATP6V1A may be more appropriately regarded as a representative molecule of lysosomal and autophagy-related modules rather than advanced as a single diagnostic biomarker. It could be combined with other lysosomal enzymes, antigen-presentation molecules, complement proteins, and inflammatory factors to construct pathway-based biomarker panels.

Among the three candidate proteins, LTF showed the most clinically relevant validation result. LTF is an iron-binding glycoprotein with antibacterial, antiviral, antioxidant, and immunomodulatory functions[31–33]. It participates in host defense by regulating iron homeostasis, suppressing excessive inflammatory responses, influencing neutrophil activation, and modulating cytokine release. In ophthalmic research, LTF is an important defense protein in tears, and altered LTF levels have been investigated in dry eye, Sjogren syndrome-related keratoconjunctivitis sicca, and other ocular surface inflammatory conditions[33]. In addition, LTF has been reported in ocular tissues and vitreous humor, suggesting that it is not restricted to the ocular surface but may participate more broadly in intraocular protection and inflammatory regulation. In the present study, LTF differed significantly between AON and CTL and between NAION and CTL and showed diagnostic utility in ROC analysis, indicating that it may reflect local ocular inflammation or tissue injury associated with optic neuropathy.

The main value of LTF lies in its ability to indicate intraocular inflammatory, defense, and tissue-injury responses associated with optic neuropathy. Its favorable performance in the comparison between AON and CTL suggests that AH LTF may reflect activation of the local immune microenvironment during AON. In addition, the links between LTF and iron homeostasis, antioxidant responses, and neutrophil-associated inflammatory regulation provide clues for understanding local protective responses after optic nerve injury. Given that clinical diagnosis usually relies on multidimensional evidence, LTF may be best positioned as a candidate molecule in AH liquid biopsy, to be integrated with serum antibodies, OCT/OCTA structural and perfusion parameters, MRI features, and other protein markers in a multimodal diagnostic model.

From a translational perspective, early diagnosis of AON remains challenging. Serum antibody testing can provide important etiological clues, but diagnostic uncertainty persists in antibody-negative patients, patients tested at different

time points, and patients with atypical phenotypes[8–10]. Imaging can demonstrate optic nerve inflammation, edema, and atrophy, but its ability to capture early molecular changes is limited. AH proteomics can serve as a complementary strategy by providing molecular-level information about the local intraocular microenvironment. The present study suggests that LTF and modules related to immune response, ribosomal translation, glycoprotein biosynthesis, and lysosomal function may participate in AON-related AH molecular changes. Future integration of these fluid biomarkers with OCT/OCTA quantitative parameters, serum antibodies, and clinical symptoms may help establish more robust multimodal diagnostic models[11–13, 34, 35].

This study has several limitations. First, the sample size was relatively limited, especially for discovery proteomics and ELISA validation, and may not fully capture the clinical heterogeneity of AON. Second, this was a single-center study, and differences in disease duration, inflammatory activity, baseline comorbidities, and pretreatment status may have influenced AH protein expression. Third, AON was not further stratified by etiological subtype, and the current conclusions therefore apply mainly to AON as an overall group. Whether AH proteomic profiles differ across antibody status or immune backgrounds remains unclear. Fourth, the CTL group consisted of patients undergoing presbyopic surgery, and differences in age, lens status, or perioperative factors may have affected the background AH proteome. Fifth, only LTF, RPSA, and ATP6V1A were validated by ELISA, and additional candidate proteins have not yet been confirmed by targeted mass spectrometry or multiplex immunoassays. Functional evidence from cellular or animal experiments is also lacking.

In summary, this study revealed molecular changes in the local ocular microenvironment associated with AON from the perspective of AH proteomics and identified LTF as a promising candidate biomarker related to optic neuropathy-associated inflammatory responses. The negative validation results for RPSA and ATP6V1A suggest that pathway or network-centered molecules identified during discovery may not directly translate into single diagnostic markers, although the protein translation stress and lysosomal functional changes they represent remain worthy of further investigation. Future studies with larger cohorts, longitudinal follow-up, multiprotein validation, and functional experiments are needed to further clarify the value of AH proteomics in the diagnosis, disease assessment, and mechanistic study of AON.

Conclusion

By combining DIA-based AH proteomic analysis with ELISA validation, this study preliminarily characterized the distinctive AH protein expression profile of patients with AON. LTF showed promising potential as a candidate biomarker in AH, suggesting that AH proteomics may provide a new approach for elucidating local pathological mechanisms and identifying fluid-based biomarkers for AON.

Future studies should further validate and extend these findings and explore their relevance to disease mechanisms and targeted therapeutic strategies.

Abbreviations

AON
autoimmune optic neuritis
NAION
non–arteritic anterior ischemic optic neuropathy
CTL
control
AH
aqueous humor

DIA
data–independent acquisition
ELISA
enzyme–linked immunosorbent assay
LC
MS/MS–liquid chromatography–tandem mass spectrometry
GO
Gene Ontology
KEGG
Kyoto Encyclopedia of Genes and Genomes
PPI
protein–protein interaction
LTF
lactoferrin
RPSA
ribosomal protein SA
ATP6V1A
ATPase H+ transporting V1 subunit A
ROC
receiver operating characteristic
BCVA
best–corrected visual acuity
IOP
intraocular pressure
AQP4
IgG–aquaporin–4 immunoglobulin G
MOG
IgG–myelin oligodendrocyte glycoprotein immunoglobulin G
GFAP
glial fibrillary acidic protein
FDR
false discovery rate.

Declarations

Competing interests

The authors declare that they have no competing interests.

Ethics approval and consent to participate

This study was approved by the Ethics Committee of the Affiliated Hospital of Nantong University and was conducted in accordance with the Declaration of Helsinki. Written informed consent was obtained from all participants or their legal representatives.

Funding

This work was supported by the National Natural Science Foundation of China (82571192 and 82571190), Jiangsu Province Frontier Technology Research and Development Program—Key Clinical Diagnosis and Treatment Technology Research Project (BF2025638), Nantong Natural Science Foundation (JC2025043).

Author Contribution

Qingyuan Mao, Min Zhang, Junfang Zhang, Jiawei Luo, Huaijin Guan and Min Ji: writing, review and editing; Qingyuan Mao and Min Zhang: writing original draft; Qingyuan Mao and Min Zhang: validation; Qingyuan Mao:software; Qingyuan Mao, Min Zhang, Shiyu Huang, and Hongwei Gu: sample collection; Huaijin Guan, Min Ji, Junfang Zhang and Jiawei Luo: project administration; Qingyuan Mao, Min Zhang, Huaijin Guan, Min Ji, Junfang Zhang and Jiawei Luo: methodology; Qingyuan Mao and Min Zhang: formal analysis; Qingyuan Mao and Min Zhang: data curation; Junfang Zhang, Jiawei Luo, Huaijin Guan and Min Ji: supervision; Huaijin Guan and Min Ji: funding acquisition.

Data Availability

All data supporting the findings of this study are available within the paper and its Supplementary Information.

References

1. BENNETT JL, COSTELLO F, CHEN JJ et al (2023) Optic neuritis and autoimmune optic neuropathies: advances in diagnosis and treatment [J]. Lancet Neurol 22(1):89–100
2. PETZOLD A, FRASER C L, ABEGG M et al (2022) Diagnosis and classification of optic neuritis [J]. Lancet Neurol 21(12):1120–1134
3. HASSAN M B, STERN C, FLANAGAN E P et al (2020) Population-Based Incidence of Optic Neuritis in the Era of Aquaporin-4 and Myelin Oligodendrocyte Glycoprotein Antibodies [J]. Am J Ophthalmol 220:110–114
4. BECK R W, CLEARY P A, ANDERSON M M et al (1992) A Randomized, Controlled Trial of Corticosteroids in the Treatment of Acute Optic Neuritis [J]. N Engl J Med 326(9):581–588
5. FARD M A, YADEGARI S, GHAHVECHIAN H et al (2019) Optical Coherence Tomography Angiography of a Pale Optic Disc in Demyelinating Optic Neuritis and Ischemic Optic Neuropathy [J]. J Neuroophthalmol 39(3):339–344
6. SUN C-B XIAOQ (2024) MA Z. Optical coherence tomography angiography of peripapillary vessel density in non-arteritic anterior ischemic optic neuropathy and demyelinating optic neuritis [J]. Front Neurol, 15
7. WEI S, TIAN G (2015) Expert Consensus on the Diagnosis and Treatment of Non-Arteritic Anterior Ischemic Optic Neuropathy in China [J]. Chin J Ophthalmol 51(5):323–326
8. WINGERCHUK D M, BANWELL B (2015) International consensus diagnostic criteria for neuromyelitis optica spectrum disorders [J]. Neurology 85(2):177–189
9. BANWELL B, BENNETT J L, MARIGNIER R et al (2023) Diagnosis of myelin oligodendrocyte glycoprotein antibody-associated disease: International MOGAD Panel proposed criteria [J]. Lancet Neurol 22(3):268–282
10. LENNON V A, WINGERCHUK D M, KRYZER T J et al (2004) A serum autoantibody marker of neuromyelitis optica: distinction from multiple sclerosis [J]. Lancet 364(9451):2106–2112
11. WATANABE M, NAKAMURA Y, MICHALAK Z et al (2019) Serum GFAP and neurofilament light as biomarkers of disease activity and disability in NMOSD [J]. Neurology, 93(13)
12. JIN R, SUN S, LIU X (2025) Immunopathology of optic neuritis and cerebrospinal fluid biomarkers for acute attack and relapse prediction [J]. Immunol Cell Biology 103(10):916–937

13. SHAH S, MARIOTTO S, FLANAGAN E P et al (2025) Neurofilament light chain levels differentiate ischemic from inflammatory optic neuropathies [J]. Multiple Sclerosis and Related Disorders, p 104
14. MURTHY K R, RAJAGOPALAN P, PINTO S M et al (2015) Proteomics of Human Aqueous Humor [J]. OMICS 19(5):283–293
15. WOLF J, RASMUSSEN D K, SUN Y J et al (2023) Liquid-biopsy proteomics combined with AI identifies cellular drivers of eye aging and disease in vivo [J]. Cell 186(22):4868–4884e4812
16. OH J W, AHN S J, JUNG J H et al (2025) Proteomic Analysis of Aqueous Humor Identified Clinically Relevant Molecular Targets for Neovascular Complications in Diabetic Retinopathy [J], vol 24. Molecular & Cellular Proteomics, 4
17. FUNAGURA N, FUJIMOTO T, TAKAHASHI E et al (2025) Large-scale proteomic analysis of aqueous humor from patients with primary open angle and exfoliation glaucoma [J]. Sci Rep, 15(1)
18. REJAS-GONZáLEZ R, MONTERO-CALLE A, PASTORA SALVADOR N et al (2024) Unraveling the nexus of oxidative stress, ocular diseases, and small extracellular vesicles to identify novel glaucoma biomarkers through in-depth proteomics [J]. Redox Biol, 77
19. WU L, AN J, LI X et al (2024) Comprehensive Proteomic Profiling of Aqueous Humor in Idiopathic Uveitis and Vogt–Koyanagi–Harada Syndrome [J]. ACS Omega 9(16):18643–18653
20. ZHANG F, GE W, RUAN G et al (2020) Data-Independent Acquisition Mass Spectrometry-Based Proteomics and Software Tools: A Glimpse in 2020 [J]. Proteomics 20:17–18
21. CANTALAPIEDRA C P, HERNáNDEZ-PLAZA A, LETUNIC I et al (2021) eggNOG-mapper v2: Functional Annotation, Orthology Assignments, and Domain Prediction at the Metagenomic Scale [J]. Mol Biol Evol 38(12):5825–5829
22. SZKLARCZYK D, KIRSCH R, KOUTROULI M et al (2023) The STRING database in 2023: protein–protein association networks and functional enrichment analyses for any sequenced genome of interest [J]. Nucleic Acids Res 51(D1):D638–D646
23. WARNER JR, MCINTOSH KB (2009) How Common Are Extraribosomal Functions of Ribosomal Proteins? [J]. Mol Cell 34(1):3–11
24. VIND A C, GENZOR A V, BEKKER-JENSEN S (2020) Ribosomal stress-surveillance: three pathways is a magic number [J]. Nucleic Acids Res 48(19):10648–10661
25. GANDO I A DIGIACOMOV, VENTICINQUE L et al (2015) The transition of the 37-kDa laminin receptor (RPSA) to higher molecular weight species: SUMOylation or artifact? [J]. Cell Mol Biology Lett, 20(4)
26. KANE B A, AN H, RAJASEKARIAH P et al (2019) Differential expression and regulation of the non-integrin 37/67-kDa laminin receptor on peripheral blood leukocytes of healthy individuals and patients with rheumatoid arthritis [J]. Sci Rep, 9(1)
27. FASSIO A, ESPOSITO A, KATO M et al (2018) De novo mutations of the ATP6V1A gene cause developmental encephalopathy with epilepsy [J]. Brain 141(6):1703–1718
28. LIU M, ZHU J, ZHENG J et al (2025) GPNMB and ATP6V1A interact to mediate microglia phagocytosis of multiple types of pathological particles [J]. Cell Rep, 44(3)
29. JIN J, MU Y, ZHANG H et al (2023) CISH impairs lysosomal function in activated T cells resulting in mitochondrial DNA release and inflammaging [J]. Nat Aging 3(5):600–616
30. WANG Z, WANG H, CHEN X et al (2021) Inhibiting ATP6V0D2 Aggravates Liver Ischemia-Reperfusion Injury by Promoting NLRP3 Activation via Impairing Autophagic Flux Independent of Notch1/Hes1 [J]. Journal of Immunology Research, 2021: 1–16
31. OKUBO K, KAMIYA M, URANO Y et al (2016) Lactoferrin Suppresses Neutrophil Extracellular Traps Release in Inflammation [J]. eBioMedicine 10:204–215

32. KRUZEL M L, ZIMECKI M, ACTOR JK (2017) Lactoferrin in a Context of Inflammation-Induced Pathology [J]. Front Immunol, 8
33. CUTONE A, ROSA L, LEPANTO MS et al (2017) Lactoferrin Efficiently Counteracts the Inflammation-Induced Changes of the Iron Homeostasis System in Macrophages [J]. Front Immunol, 8
34. LEE G I, PARK K A, OH S Y et al (2020) Peripapillary and parafoveal microvascular changes in eyes with optic neuritis and their fellow eyes measured by optical coherence tomography angiography: an Exploratory Study [J]. Acta Ophthalmol 99(3):288–298
35. SYC S B SAIDHAS, NEWSOME S D et al (2012) Optical coherence tomography segmentation reveals ganglion cell layer pathology after optic neuritis [J]. Brain 135(2):521–533

Figures

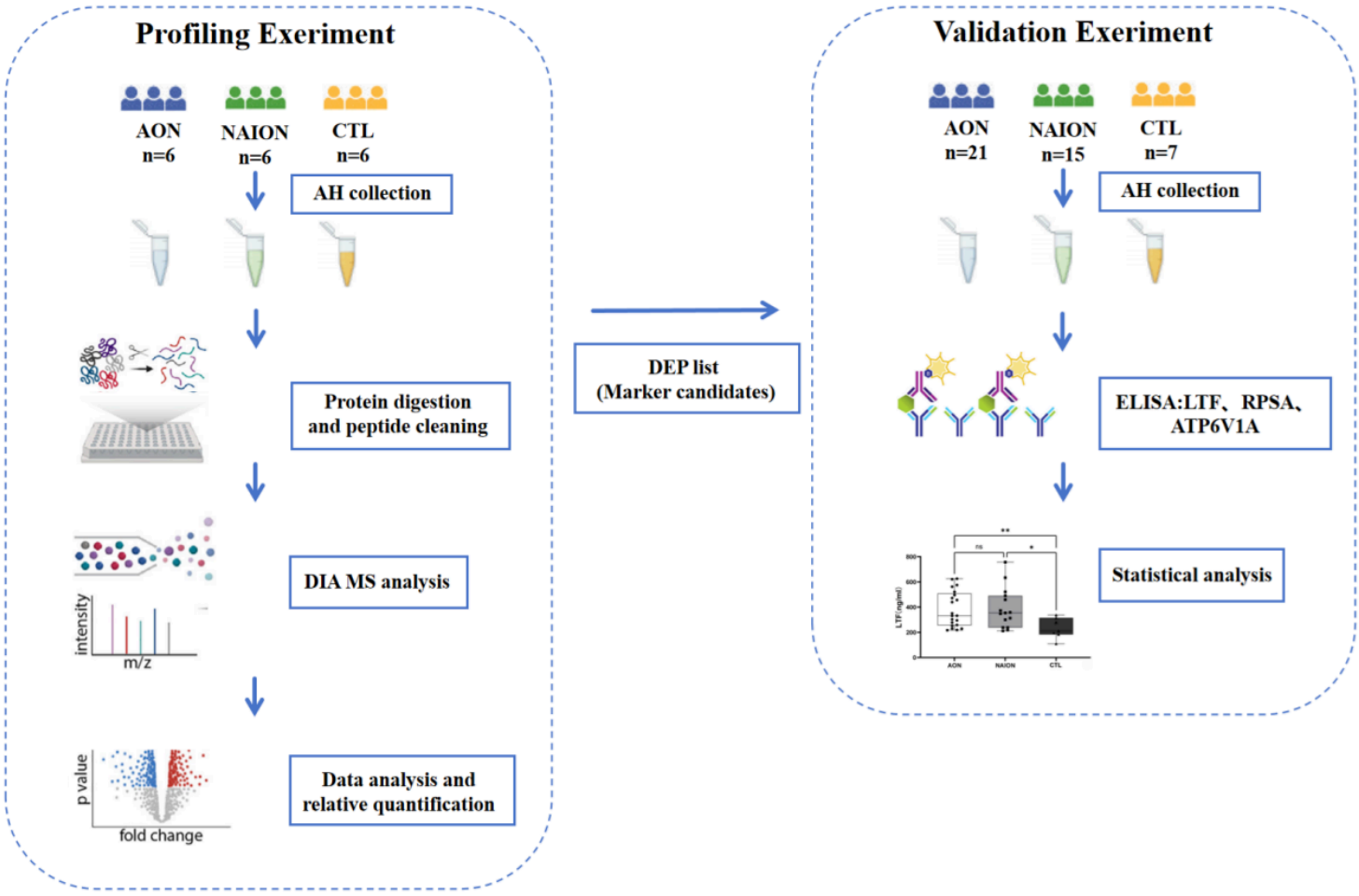


Figure 1

Proteomic workflow. The discovery experiment included AH collection, low-abundance protein enrichment, trypsin digestion, DIA LC-MS/MS proteome profiling, DIA-NN-based identification and quantification, differential protein analysis, GO/KEGG/PPI network analysis, and candidate protein selection. Candidate proteins were subsequently evaluated in the validation experiment using ELISA, followed by statistical analysis and ROC curve assessment.

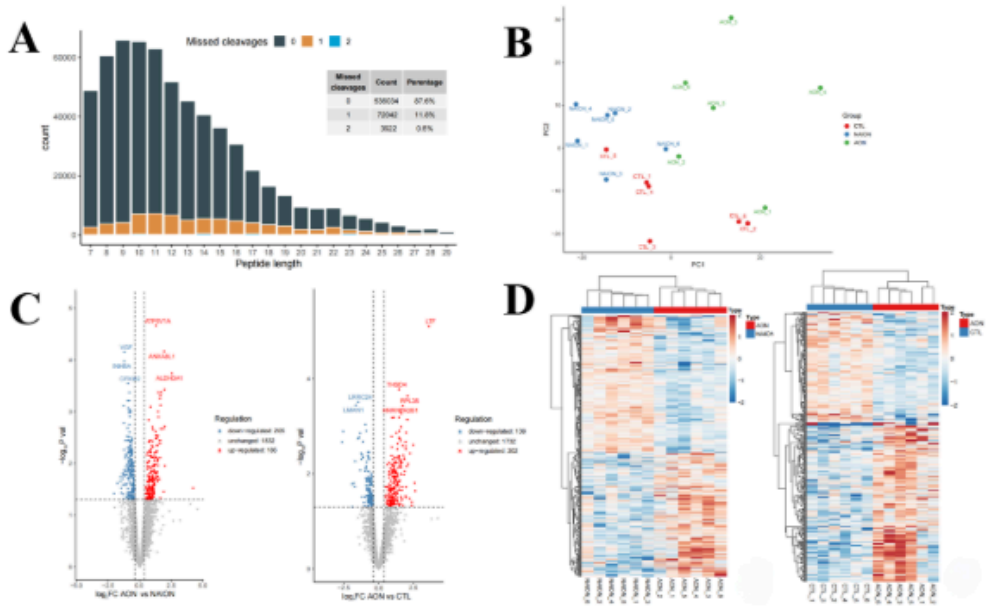


Figure 2

Proteomic quality control, principal component analysis, volcano plots, and heatmaps. (A) Peptide length distribution. DIA analysis identified 4,264 proteins. (B) Principal component analysis of the global protein expression profiles among the three groups. NAION and CTL samples showed clear intragroup clustering, whereas AON samples showed a relatively broader distribution, possibly reflecting the complex etiology of AON. The intergroup differences indicate biological heterogeneity among the three groups. (C) Volcano plots of differentially expressed proteins. Using fold change > 1.3 or < 0.77 with adjusted p < 0.05 as the screening criteria, 391 differentially expressed proteins were identified between AON and NAION, including 186 upregulated and 205 downregulated proteins. A total of 341 differentially expressed proteins were identified between AON and CTL, including 202 upregulated and 139 downregulated proteins. (D) Z-score-normalized heatmaps of significant proteins showing distinct clustering patterns between groups.

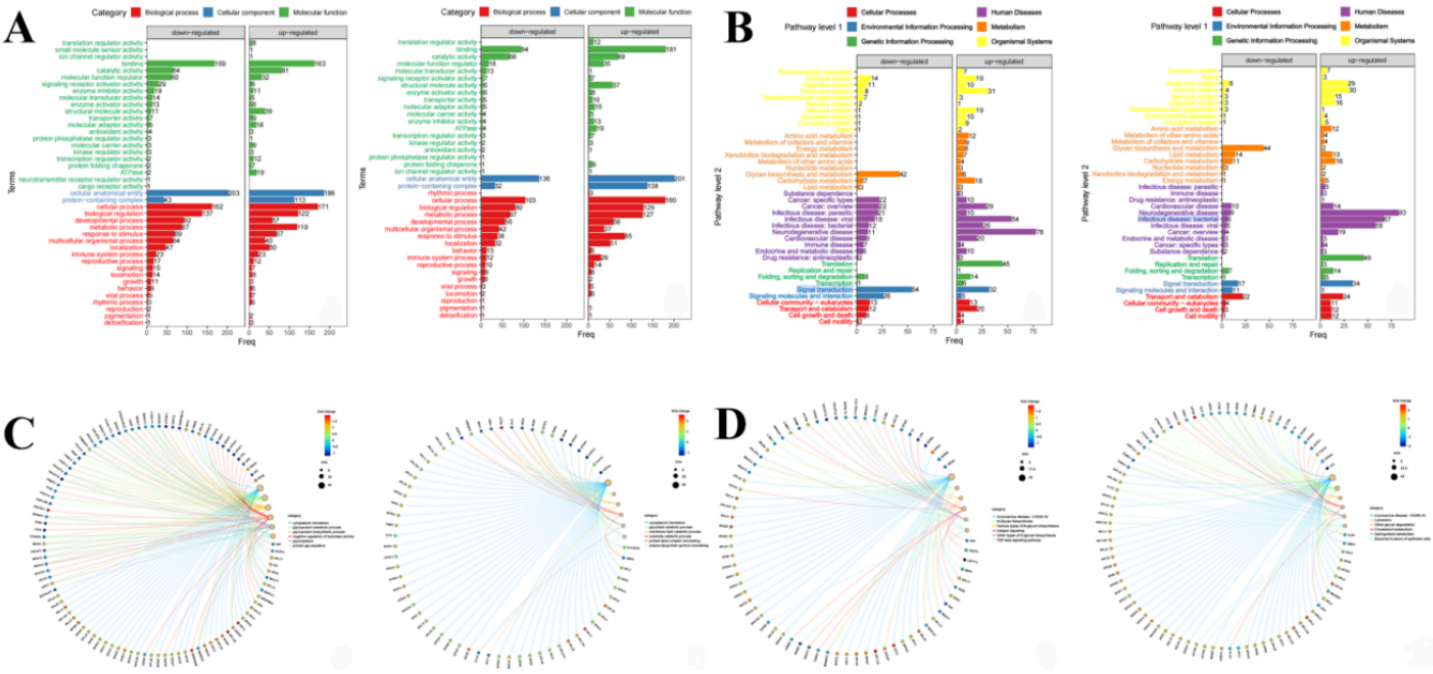


Figure 3

GO annotation and KEGG pathway enrichment analysis. (A) GO annotation describes the functional composition of differentially expressed proteins across biological process, cellular component, and molecular function categories. Differential proteins were mainly involved in response to stimulus, immune processes, catalytic activity, and signaling receptor activator activity. (B) KEGG pathway analysis based on the KEGG PATHWAY database showed that differential proteins were mainly associated with neurodegenerative diseases, glycan biosynthesis and metabolism, immune system pathways, and signal transduction. (C) GO enrichment gene-pathway network. Differentially expressed proteins were mainly involved in glycoprotein biosynthesis, enzyme inhibitor activity, signaling receptor regulatory activity, calcium ion binding, cell adhesion molecule binding, and carbohydrate metabolism. (D) KEGG enrichment gene-pathway network. Differentially expressed proteins were mainly associated with glycan biosynthesis, ganglioside biosynthesis series, lysosomes, and glycan degradation.

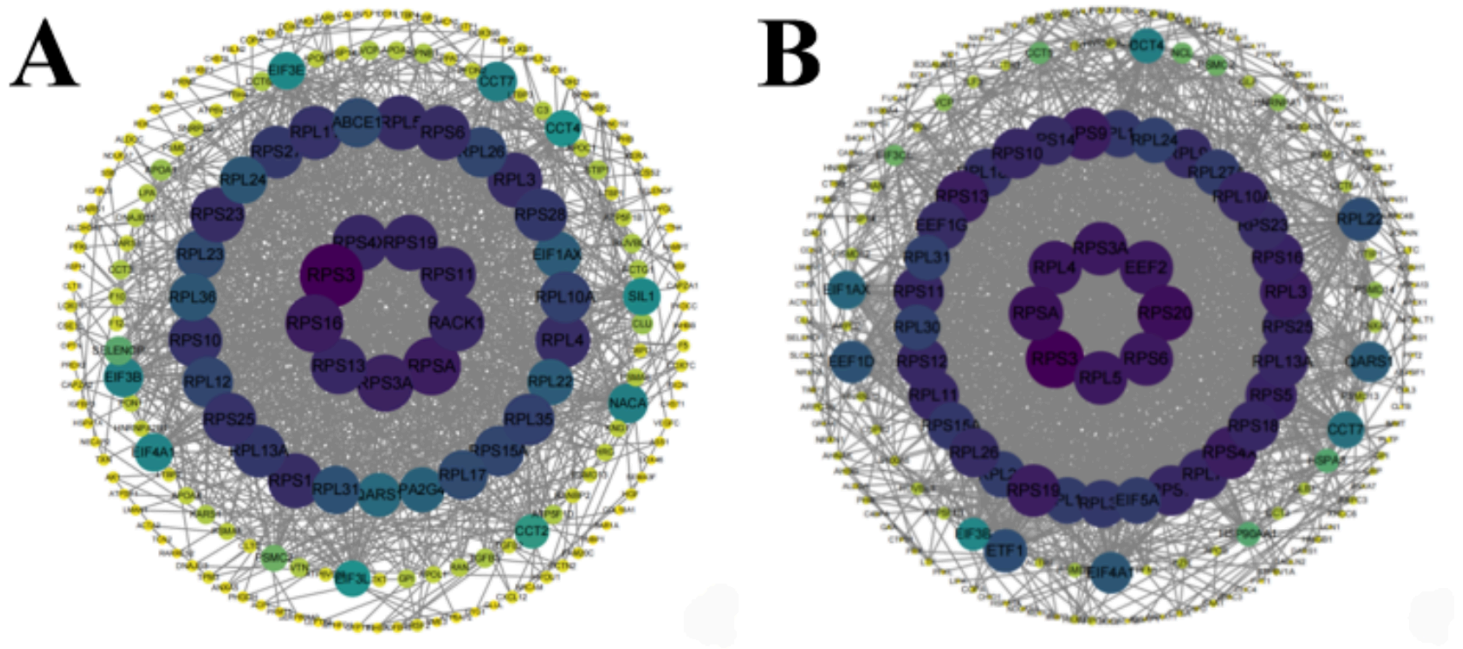


Figure 4

PPI network analysis of AON-related differential proteins. (A) PPI network of differentially expressed proteins between AON and NAION. Node size and color reflect connectivity or relative importance in the network, with ribosome-related proteins forming the core region. (B) PPI network of differentially expressed proteins between AON and CTL. Highly connected proteins in the network may represent key molecular nodes in the AH proteomic changes associated with AON.

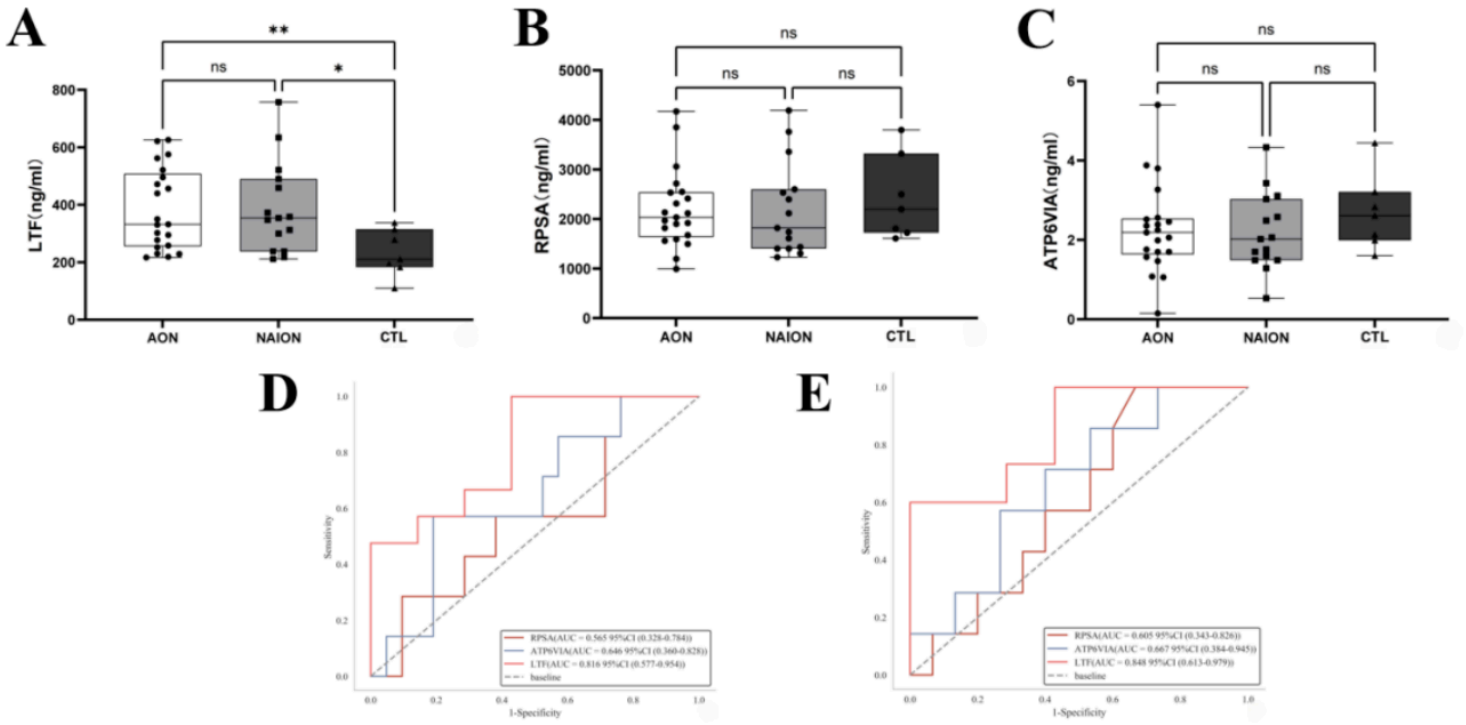


Figure 5

ELISA validation and ROC curve analysis of candidate proteins. (A-C) Expression levels of LTF, RPSA, and ATP6V1A in the validation cohort. (D, E) ROC curves of the three proteins for AON versus CTL and NAION versus CTL comparisons. LTF showed better diagnostic performance in the AON versus CTL and NAION versus CTL comparisons, whereas RPSA and ATP6V1A showed relatively limited discriminative ability.

Supplementary Files

This is a list of supplementary files associated with this preprint. Click to download.

- atp6v1.xlsx
- Lactoferrin.xlsx
- LAMR1RPSA.xlsx
- Table1a.MSidentifiedproteindetail.xls
- Table1b.MSidentifiedpeptidedetail.xls